Polymer Degradation and Stability 112 (2015) 122–131

Contents lists available at ScienceDirect

Polymer Degradation and Stability

journal homepage: www.elsevier.com/locate/polydegstab

Quantitative determination of species production from phenol-formaldehyde resin pyrolysis

Hsi-Wu Wong [a, *], Jay Peck [b], Robin E. Bonomi [b], James Assif [b], Francesco Panerai [c], Guillaume Reinisch [d], Jean Lachaud [e], Nagi N. Mansour [f]

[a] Department of Chemical Engineering, University of Massachusetts Lowell, Lowell, MA, 01854, USA
[b] Center for Aero-Thermodynamics, Aerodyne Research, Inc., Billerica, MA, 01821, USA
[c] Department of Mechanical Engineering, University of Kentucky, Lexington, KY, 40506, USA
[d] Center for Predictive Engineering and Computational Sciences, University of Texas at Austin, Austin, TX, 78712, USA
[e] University Affiliated Research Center, University of California at Santa Cruz, Moffett Field, CA, 94035, USA
[f] NASA Ames Research Center, Moffett Field, CA, 94035, USA

ARTICLE INFO

Article history:
Received 14 July 2014
Received in revised form
16 December 2014
Accepted 22 December 2014
Available online 31 December 2014

Keywords:
Phenol-formaldehyde resin
Pyrolysis
Reaction kinetics
Species production
Gas chromatography

ABSTRACT

Batch pyrolysis of a commercial resole type phenol-formaldehyde resin was performed using a step-wise heating procedure in a temperature increment of 50 K from 320 to 1290 K. A resin sample of 50 mg was loaded in a reactor assembly specifically designed and built for this study. Mass loss was measured after each 50 K step and the production of pyrolysis products was quantified using gas chromatography techniques. The overall mass loss from the samples reached 39.2% after the entire procedure. Three major product families were identified: 1) water is the most dominant product at a pyrolysis temperature below 800 K; 2) phenol derivatives (aromatic alcohols) have significant yields at a pyrolysis temperature between 500 and 850 K; 3) permanent gases such as hydrogen, methane, carbon monoxide, and carbon dioxide have the highest yields at a temperature above 800 K. Minor products observed include aromatics, which are formed between 700 and 850 K, and C_2 to C_4 light hydrocarbons, which are only formed above 800 K and peak at 1000 K.

1. Introduction

Pyrolysis of phenol-formaldehyde resins is one of the most common processes to produce amorphous carbon or carbon/carbon composites [1–4]. During pyrolysis, resin matrix converts into carbon, releasing gaseous products. The internal pressure generated from these pyrolysis products, however, poses a potential threat to the structure of carbon/carbon composites [2–4]. For this reason, one needs to obtain a detailed understanding of the decomposition kinetics of phenol-formaldehyde resins to harness the process. Similarly, when designing ablative and friction materials using phenol-formaldehyde resins for aerospace applications, in-depth knowledge of the pyrolysis kinetics is also essential for obtaining optimal performance and accurate materials response predictions [5–9].

Many experimental studies have been performed to understand the pyrolysis kinetics of phenol-formaldehyde resins. Three families of techniques have been used. Thermal analytical techniques, including thermogravimetric analysis (TGA), differential scanning calorimetry (DSC), or differential thermogravimetry (DTG), provide sample weight loss and heat flow information as a function of temperature [2,3,10–15]. These methods, although valuable in determining the enthalpies of the pyrolysis reactions and the overall mass loss, do not give detailed speciation information, necessary for the construction of detailed pyrolysis reaction mechanisms. Infrared (IR) spectroscopy techniques, such as Fourier transform infrared spectroscopy (FTIR), are used to analyze structural changes of the phenolic resin during pyrolysis [1,4,12,15–20]. Qualitative or semi-quantitative speciation information can be derived, especially coupled with thermal analytical methods, but it is difficult to obtain quantitative product yields over a wide temperature range. Gas chromatography (GC) techniques, such as pyrolysis gas chromatography mass spectrometry (Py-GC-MS) [4,13,19,21–26], provide detailed speciation information. However, introduction of the pyrolysis products into the GC systems

* Corresponding author.
E-mail address: HsiWu_Wong@uml.edu (H.-W. Wong).

http://dx.doi.org/10.1016/j.polymdegradstab.2014.12.020
0141-3910/

without loss is challenging, especially for high temperature reactions where condensation of the volatile products is suspected to take place in the transfer lines.

Although experimental limitations exist, it is generally accepted that pyrolysis of phenol-formaldehyde resins can be divided into three major stages, as proposed by Trick et al. [1,2]. The first stage involves crosslink formation as a result of condensation reactions to produce water and heavier aromatic species, which takes place in a temperature range between 550 and 800 K. The second stage involves crosslink breaking, forming light gases, such as methane, carbon monoxide and carbon dioxide, in a temperature range between 700 and 1100 K. The last stage involves the charring of the remaining resin through the formation of hydrogen gas at a temperature above 850 K. While these stages generally explain available experimental findings in the literature, a detailed chemical kinetic mechanism that can quantitatively express the temperature-dependent species production of phenol-formaldehyde resin pyrolysis is still lacking. One of the key challenges is limited available data on the detailed and quantitative species production under a wide range of conditions, such as reaction temperature.

Only few experimental studies attempted to quantitatively determine yields of detailed pyrolysis products over a wide range of temperature. The experiment performed by Sykes [21] more than 40 years ago remains to be the one with the most comprehensive data. In Syke's study, phenol-formaldehyde resin samples were heated in a pyrolyzer attached to the entrance port of a gas chromatograph. Approximately 7 mg of material was heated for 10 s before the sample was immediately quenched. The starting temperature was 298 K, and it was increased by 50 K every time when the process was repeated. Mole fractions of the gaseous products were determined as a function of temperature, as reproduced in Fig. 1.

In this work, we provide a comprehensive, quantitative speciation data set for phenol-formaldehyde resin pyrolysis over a wide range of reaction temperature (320–1290 K). We employed gas chromatography methods because they are the most promising for species identification and quantification according to previous literature studies. Thermogravimetric analysis results were also used for comparison. To overcome known limitations of the GC techniques, we designed and constructed a batch reactor system. The uniqueness of our reactor system is that everything produced in the reactor was collected without loss and was quantitatively analyzed, thus avoiding the issue of sample loss in typical GC techniques. Our work provides critical information to advance the understanding of reaction kinetics of phenol-formaldehyde resin pyrolysis. The design of this original reactor system and the results of the pyrolysis experiments performed using this set-up are presented in the following sections.

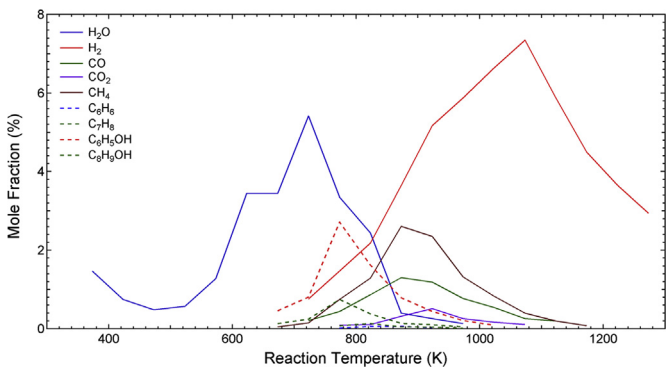

Fig. 1. Product distribution from the decomposition of a phenolic formaldehyde resin at a heating rate of 10 K/min, reported by Sykes [21].

2. Experimental techniques

2.1. Reactor design

A batch reactor system was designed and built to carry out the pyrolysis experiments. The design of the reactor assembly is shown in Fig. 2. The reactor section was made of quartz, taking advantage of its high temperature capability and good thermal shock resistance. The rest of the reactor system was made of stainless steel. Two thermocouples were used to monitor and record temperatures; one inside the sample and the other at the reactor top near the interface between the quartz reactor and the stainless steel fitting. During the experiments, the quartz reactor was inserted into a heating furnace, custom-made from high-temperature heating wires and castable ceramics, as shown in Fig. 3. The furnace temperature was controlled with a PID controller. The condenser was positioned in a liquid nitrogen bath, allowing the pyrolysis products to move toward the condenser section by thermal diffusion, where most volatile species condense. The reactor system was designed to cool down as quickly as possible outside the reaction zone. Lower temperature outside the reaction zone also reduces system pressure and allows larger species with low volatility to condense, both of which lower the effect of homogeneous gas phase chemistry.

2.2. Experimental procedure

The experimental protocol employed in this study partially replicated the protocol used by Sykes [21]. The main goal is to store and analyze pyrolysis products within 50 K temperature increments (that is, between 320 and 370 K, 370 and 420 K, etc.) rather than attempting on-the-fly measurements, which are susceptible to sample loss due to condensation of pyrolysis products in the reactor and transfer lines. There are two advantages to our approach: (1) the sample's mass can be measured at each step, avoiding the need of using a thermogravimetric analyzer where volatile vapors may condense in the system, and (2) the volatile pyrolysis products that condense on the wall of the reactor assembly can be easily collected by liquid extraction and analyzed.

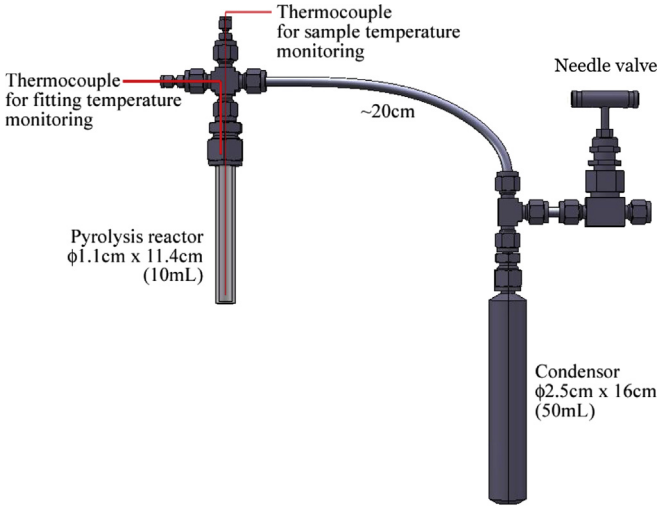

Fig. 2. 3D model of the batch reactor with key dimensions.

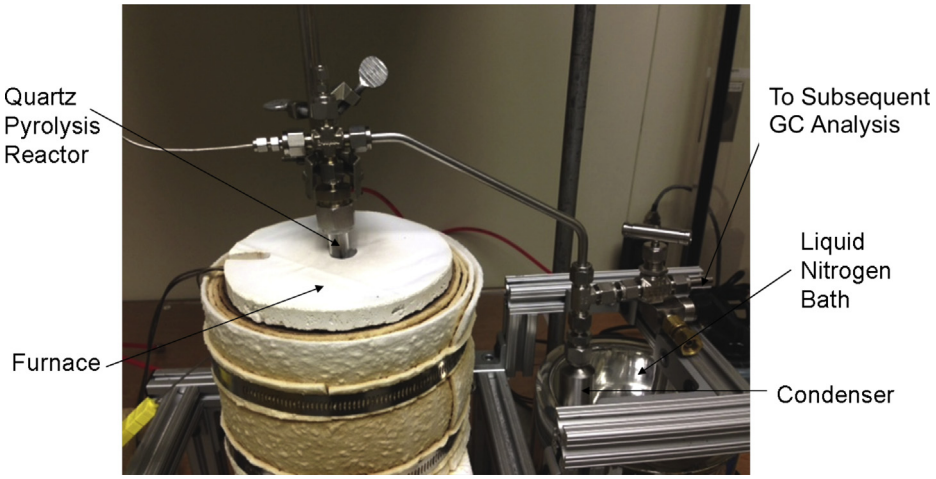

Fig. 3. The batch reactor system for the pyrolysis experiments.

Resole type phenol-formaldehyde resin samples acquired from Durez Corporation were firstly cured at 450 K for 30 min (as instructed by the sample supplier). 50 mg of cured samples were loaded in the quartz reactor. The reactor was then vacuumed to below 13 Pa (0.1 torr) to minimize any potential gas-phase chemistry. The needle valve of the reactor was then closed, and the reactor assembly was inserted into the furnace pre-set at a desired reaction temperature. The sample typically reached the furnace temperature within 2–10 min following insertion. The reactor was kept at the target temperature for 1 h to ensure that pyrolysis reactions at this temperature were near completion. The reactor was then quenched in a cold water bath back to room temperature, typically within 2 min. Examples of measured sample temperature as a function of time during our experiments can be seen in Fig. 4.

The internal pressure in the reactor after the reaction provides a good estimate of the amount of pyrolysis products formed in the gas phase. To measure this quantity, the reactor assembly was attached to a pre-vacuumed stainless steel line with an internal diameter of 6.35 mm. The vacuum line was connected to a MKS 122A pressure gauge and a MKS PDR-0-1 digital readout for accurate pressure measurements. The needle valve of the reactor assembly was then opened, and the pressure reading was used to calculate the original reactor pressure based on the volumes of the reactor assembly (approximately 73 mL) and the vacuum line (approximately 32 mL). Between 650 and 1950 Pa (5–15 torr) of n-pentane vapor, which was used as an external standard for analyzing gaseous products, was then added to the reactor from a separate port connected to the vacuum line. The amount of n-pentane vapor added was determined by the additional pressure increase measured from the pressure gauge. The needle valve was then closed and the reactor assembly was taken for GC analysis.

Identification of pyrolysis products was performed by an Agilent 6890N GC system equipped with a 5975 mass selective detector (MSD) using preliminary pyrolysis results obtained prior to the step-wise experiments. For species quantification, the reactor assembly was attached to a 4.5 mL pre-vacuumed chamber with a sample extraction port that allows gas-tight syringes to extract samples. Once the reactor assembly and the vacuum chamber were connected, the needle valve of the reactor assembly was opened to allow the sample to flow into the vacuum chamber before the valve was closed. A 2 mL gas phase sample was taken using a gas-tight syringe (Supelco) through the sample extraction port of the vacuum chamber. The sample was then immediately injected into an Agilent 7820A GC equipped with a thermal conductivity detector (TCD) and a Restek ShinCarbon ST 80/100 packed column (with an internal diameter of 2 mm and a length of 2 m) to quantify permanent gases. High purity helium (Airgas) with a constant flow pressure of 12 psi was used as the carrier gas in the column. The temperature of the inlet was set at 225 °C. The GC oven was programmed with the following temperature regime: hold at 35 °C for 2 min, ramp to 50 °C at 5 °C/min, hold at 50 °C for 3 min, ramp to 230 °C at 15 °C/min, and hold at 230 °C for 10 min. The detector temperature was set at 200 °C, with a reference gas flow rate of 15 mL/min and a makeup gas flow rate of 5 mL/min.

After the sample was injected, the reactor assembly was again connected to the vacuumed chamber. The same sample extraction procedure was repeated, except that a 1 mL gas phase sample was taken for an injection into the GC/MSD system equipped with a

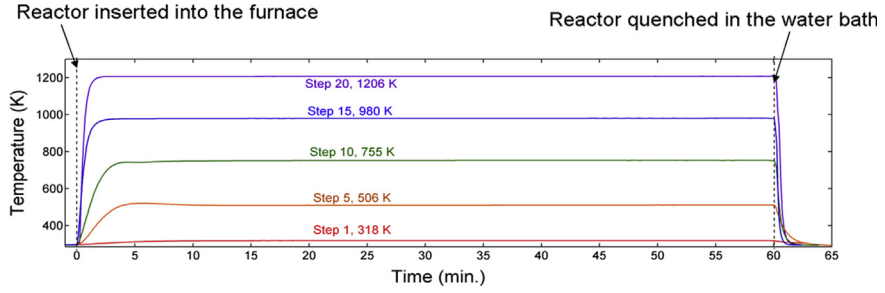

Fig. 4. Measured sample temperature as a function of time for five different steps in the pyrolysis experiments.

Restek Q-Bond PLOT column (with an internal diameter of 0.32 mm, a length of 30 m, and a film thickness of 10 μm) to quantify water vapor. The carrier gas (high purity helium) for this analysis was set at a constant flow rate of 3 mL/min. The temperature of the inlet was set at 250 °C. The GC oven was programmed with the following temperature regime: start at 35 °C, ramp to 50 °C at 15 °C/min, ramp to 100 °C at 5 °C/min, hold at 100 °C for 3 min, ramp to 250 °C at 25 °C/min, and hold at 250 °C for 4 min.

The extraction procedure was repeated for the third time to extract a 1 mL gas phase sample for an injection into the Agilent 7820A GC equipped with a flame ionization detector (FID) and a Restek Q-Bond PLOT column to quantify light ($<C_9$) hydrocarbons. High purity helium carrier gas was maintained at a constant pressure of 14.931 psi. The temperature of the inlet was set at 250 °C. A split of the carrier gas (1:10) was used. The GC oven was programmed with the following temperature regime: start at 35 °C, ramp to 50 °C at 15 °C/min, ramp to 100 °C at 5 °C/min, hold at 100 °C for 3 min, ramp to 250 °C at 25 °C/min, and hold at 250 °C for 4 min. The FID temperature was set at 300 °C, with a hydrogen gas flow rate of 30 mL/min and a air flow rate of 400 mL/min.

After these gas phase GC analysis, the reactor assembly was disassembled. The quartz reactor was capped to avoid penetration of ambient air humidity into the sample. To quantify liquid phase products in the condenser, 15 mL of dichloromethane were used to rinse the stainless steel sections of the reactor assembly. At the same time, 5–10 mg of biphenyl were added into the solution as an external standard for the quantification of liquid products. The solution was collected for further GC analysis using FID and a Restek Rxi®-5Sil MS capillary column (with an internal diameter of 0.25 mm, a length of 30 m, and a film thickness of 0.25 μm) to analyze aromatics and aromatic alcohol (phenol derivatives) compounds. For this analysis, 5 μL of the solution was injected, and the temperature of the GC inlet was set at 300 °C. The carrier gas was set at a constant pressure of 4.87 psi, with a split of the carrier gas (high purity helium) at 1:10. The GC oven was programmed with the following temperature regime: hold at 30 °C for 5 min, ramp to 180 °C at 7.5 °C/min, hold at 180 °C for 5 min, ramp to 285 °C at 15 °C/min, and hold at 285 °C for 8 min.

The above GC analytical techniques allow detection and quantification of any hydrocarbon or permanent gas species with a molecular weight smaller than approximately 400 g/mol.

Lastly, an electronic balance (Ohaus AV264C) with a repeatability of 0.1 mg was used to measure the weight of the capped quartz reactor for the determination of mass loss after each 50 K increment. The stainless steel reactor assembly was cleaned with dichloromethane and then dried in a convection oven at 373 K for 30 min before being reassembled for the next run. This elementary procedure was then repeated using the same sample, with the furnace temperature set at 50 K higher than the previous run. The first experiment in this step-wise procedure started with a furnace temperature of 323 K, and the procedure was repeated with 50 K increments until a furnace temperature of 1373 K.

In this work, three sets of pyrolysis experiments with an identical step-wise procedure were performed to confirm reproducibility. Standard deviations of the three experiment sets were used as error bars in our figures.

3. Results and discussion

3.1. GC calibration

GC calibration for each of the analytical techniques was performed by analysis of reference chemical standards, which allowed response factors for any detectable species to be calculated. Linear responses were obtained in each case. The response factors were used to quantify H_2, CO, CH_4, CO_2, C_2H_4, and C_2H_6 using GC/TCD, H_2O using GC/MSD, and all hydrocarbon compounds using GC/FID. Details of how GC calibrations were performed and how response factors were obtained are provided in the Supplemental Information section.

3.2. Reaction temperature, mass yields, and pressure

Fig. 5 shows measured sample temperature against furnace set temperature during the pyrolysis experiments. The ferrule temperature, which is the temperature at the interface between the quartz reactor and the stainless steel assembly, was also measured and plotted in the figure. As illustrated in the figure, measured sample temperatures are linearly dependent on the furnace set temperature, but usually lower by between 3 and 80 K, depending on the set temperature. The ferrule temperature never exceeded 450 K, which suggests that the temperature gradient above the sample is large and any homogeneous gas phase chemistry above the pyrolysis zone is significantly quenched due to low headspace temperatures.

The mass yields quantified by GC are plotted in Fig. 6 against mass loss measured by the electronic balance. As shown in the figure, the mass loss of the phenol-formaldehyde resin peaks at 750 K. According to our GC analysis, water is the dominant product below 800 K. As the reaction temperature increases, liquid products extracted from the dichloromethane solution, containing mostly aromatics and aromatic alcohols, start to form in a temperature range between 500 and 850 K. Above 800 K, permanent gases are the major products. Fig. 6 also shows that at lower temperatures, the mass yields from the GC measurements were lower than the mass loss measured from the balance. This is because water is the most dominant species in this temperature range, and water quantification using GC is subject to large errors due to exposure to ambient humidity throughout the analytical process. At higher temperatures, mass loss is very minor, and it is challenging for the electronic balance to accurately determine such a small mass difference, resulting in mass yields from the GC measurements higher than the mass loss measured from the balance. In general, however, the agreement between the two measurements is good, within 0.5 mg. The accumulated mass loss as a function of reaction temperature, derived from Fig. 6, is shown in Fig. 7. As illustrated in the figure, 39.2% of the initial sample mass is lost by pyrolysis after a reaction temperature of 1290 K.

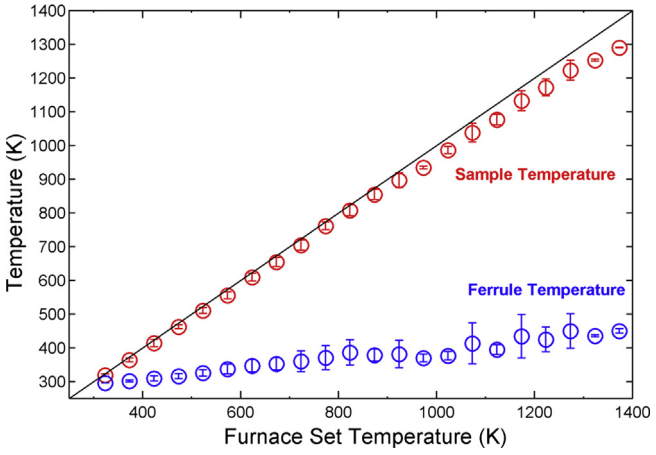

Fig. 5. Comparison of measured sample and ferrule temperatures against furnace set temperature in the pyrolysis experiments.

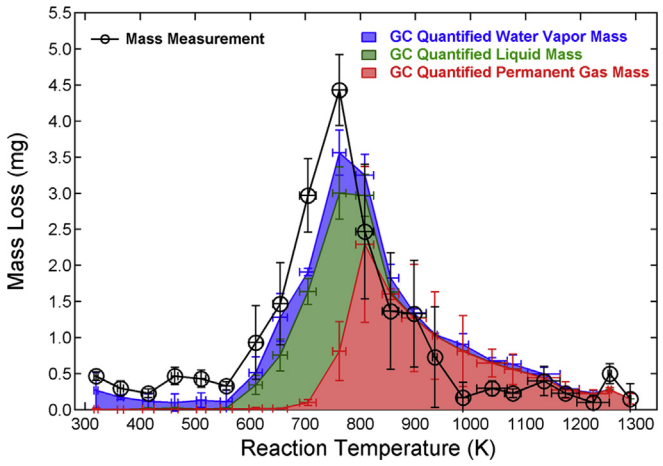

Fig. 6. The mass yields as a function of temperature from the pyrolysis experiments.

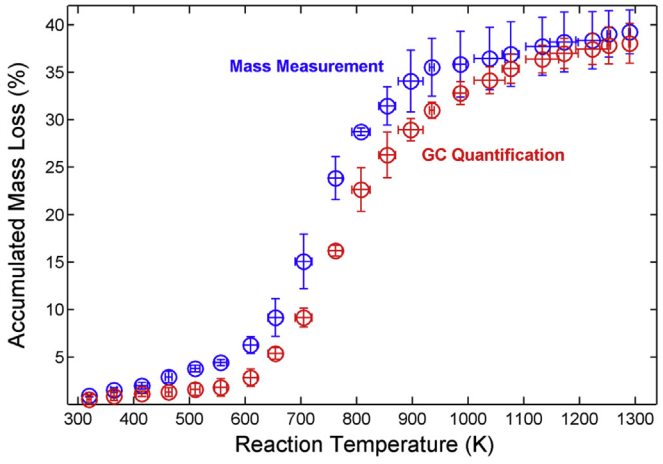

Fig. 7. The accumulated mass yields from the pyrolysis experiments.

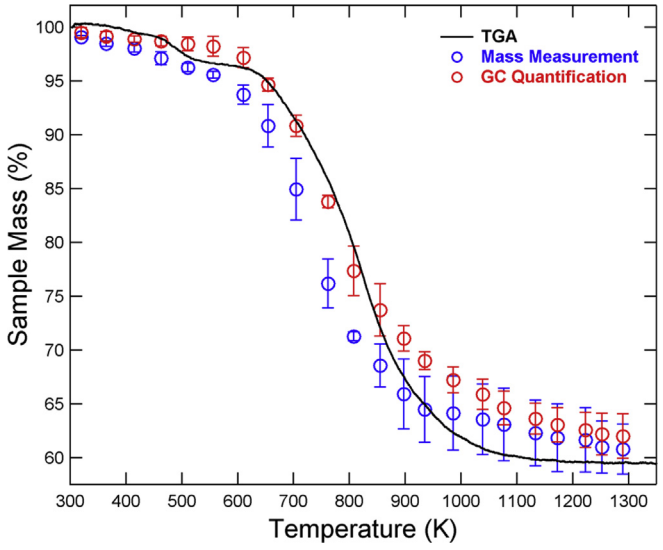

Fig. 8. The accumulated mass yields from the pyrolysis experiments.

A validation of the stepwise mass loss measurements was performed by thermo-gravimetric analysis (TGA). We used a commercial TGA system (Thermal Analyzer STA 449 F3 Jupiter, Netzsch, Burlington, MA) to test a sample of approximately 4 g, at temperatures up to 1670 K. The measurement was performed at a heating rate of 10 K/min in inert atmosphere. The chamber was evacuated to a base pressure of 10^{-2} Pa and filled with Ar gas up to room atmosphere. During the heating phase a constant flow of Ar at 200 ml/min was supplied, preventing the infiltration of external oxidants and providing adequate flushing of the pyrolysis gases. The instrument was calibrated prior to the test under the same operating conditions.

The measured mass loss obtained from TGA is plotted in Fig. 8 against the mass loss measurements obtained from the laboratory experiments (with the electronic balance and gas chromatography, respectively). As illustrated in the figure, all three mass loss measurements are agreeable.

The reactor pressure measured at room temperature after each pyrolysis step is shown in Fig. 9. As illustrated in the figure, the final reactor pressure peaked at a pyrolysis temperature of 900 K and dropped afterwards. The increase and drop in this pressure did not exactly follow the mass loss trend in Fig. 6: pressure plot peaked at a higher temperature (900 K) than the mass loss plot (750 K) did. This suggests that at a reaction temperature near 900 K, similar or even less amount (in terms of mass) of sample is pyrolyzed, but smaller species, such as hydrogen gas, is formed, resulting in higher molar yields and thus higher system pressure.

3.3. Species yields

In this study, four different families of pyrolysis products were identified by GC analysis. A representative chromatograph for the 855 K decomposition step is shown in Fig. 10. These families of products include (1) water vapor and permanent gases, such as hydrogen (H_2), carbon monoxide (CO), carbon dioxide (CO_2), methane (CH_4); (2) light hydrocarbons, such as ethene (C_2H_4), ethane (C_2H_6), propene (C_3H_6), propane (C_3H_8), butene (C_4H_8), and butane (C_4H_{10}); (3) aromatics, such as benzene (C_6H_6), toluene (C_7H_8), and xylene (C_8H_{10}); (4) aromatic alcohols (phenol derivatives), such as phenol (C_6H_6O), cresol (C_7H_8O), xylenol (dimethylphenol, $C_8H_{10}O$), and trimethylphenol ($C_9H_{12}O$). All identified products are consistent with previous experimental findings by Sykes and Trick et al. [1,2,21].

The molar and mass yields of pyrolysis products at each pyrolysis temperature are summarized and tabulated in Tables 1 and 2.

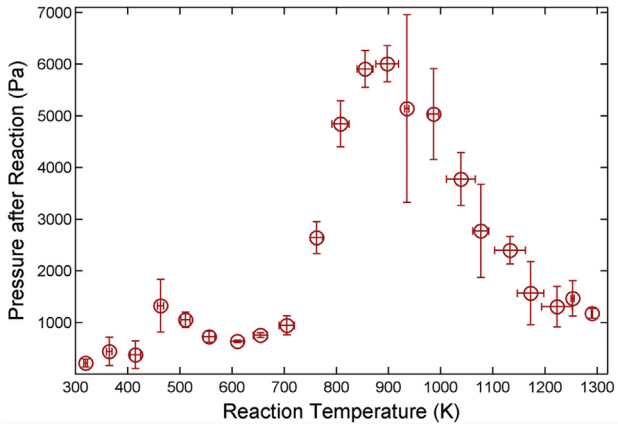

Fig. 9. The final pressure measured at room temperature after each run as a function of reaction temperature.

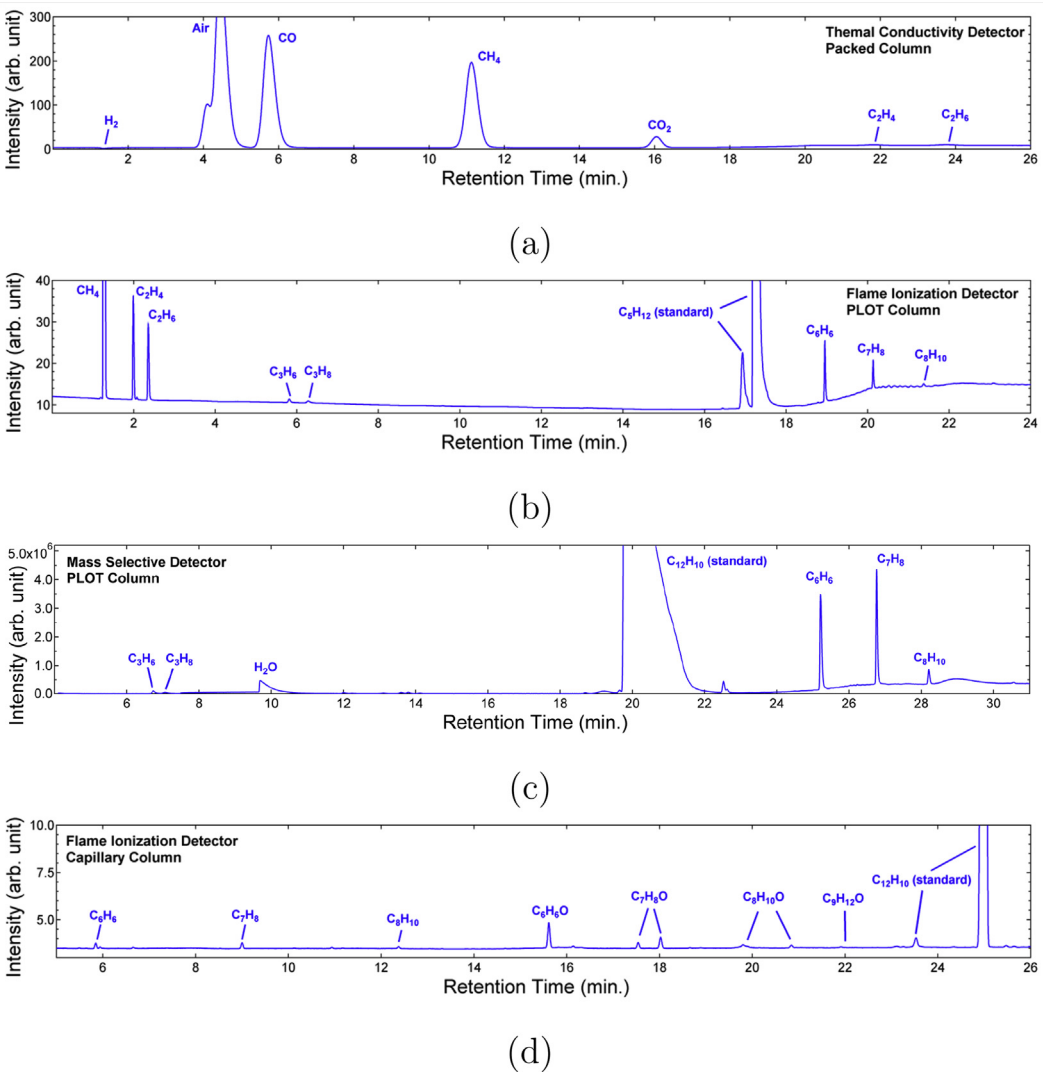

Fig. 10. A chromatograph from our gas chromatography (GC) analysis using (a) packed column with TCD, (b) PLOT column with FID, (c) PLOT column with MSD, and (d) capillary column with FID. The reaction temperature was 855 K.

The temperature dependent product yields are also plotted in Figs. 11 to 14. As illustrated in Fig. 11, water vapor is the main product at low temperatures (<800 K), and permanent gases, including hydrogen, methane, CO, and CO_2, become more dominant at higher (> 800 K) temperatures. Hydrogen gas is the most abundant product at temperatures above 900 K, and its molar yields account for most of the pressure increase at high pyrolysis temperatures (as shown in Fig. 9). In addition to permanent gases, light hydrocarbons, such as C_2 to C_4 hydrocarbons, are also produced from phenolic resin pyrolysis, as shown in Fig. 12. Interestingly, the yields of these species dramatically increase at temperatures above 800 K and then drop after 1000 K. Their yields are low compared to permanent gases. The production of these hydrocarbons were not reported in Sykes' experiments, and they may be formed via radical recombination reactions in the colder zones of the reactor headspace. The yields of aromatic species are shown in Fig. 13. Their yields are only significant at reaction temperatures between 700 and 850 K, which are comparable with yields of light hydrocarbons except ethane. At a reaction temperature above 850 K, the yields of these aromatic products become negligible. Finally, phenol and its derivatives, as shown in Fig. 14, are significant in a temperature range between 500 and 850 K. Among them, phenol and cresol have the highest yields.

4. Conclusion

A batch reactor system was designed and built specifically for this study to fully collect and quantify products from phenol-formaldehyde resin pyrolysis. The experimental protocol was based on a step-wise heating procedure in a 50 K increment to pyrolyze a 50 mg sample from 320 to 1290 K. The pyrolysis products were identified and quantified using gas chromatography techniques. Key conclusions from our experiments are:

- The overall mass loss during a commercial resole type phenol-formaldehyde resin pyrolysis is 39.2% after a reaction temperature of 1290 K;
- Water is the most dominant pyrolysis product below a pyrolysis temperature of 800 K;
- Phenol derivatives (aromatic alcohols) are significant at a pyrolysis temperature between 500 and 850 K;

Table 1
Molar yields of pyrolysis products versus pyrolysis temperature.

Pyrolysis temperature (K)	Molar yields (mmol)						
	H_2O	H_2	CH_4	CO	CO_2	C_2H_4	C_2H_6
320	$1.42\cdot10^{-2}$				$8.63\cdot10^{-3}$		
364	$9.64\cdot10^{-3}$				$2.83\cdot10^{-3}$		
415	$5.66\cdot10^{-3}$				$8.27\cdot10^{-3}$		
463	$3.84\cdot10^{-3}$		$1.63\cdot10^{-5}$	$3.16\cdot10^{-5}$	$7.45\cdot10^{-3}$		
511	$6.53\cdot10^{-3}$		$1.55\cdot10^{-5}$	$1.69\cdot10^{-4}$	$3.77\cdot10^{-3}$		
556	$4.99\cdot10^{-3}$		$2.55\cdot10^{-5}$	$1.47\cdot10^{-4}$	$7.63\cdot10^{-3}$		
610	$9.64\cdot10^{-3}$		$7.18\cdot10^{-5}$	$9.22\cdot10^{-5}$	$1.67\cdot10^{-2}$		
654	$2.91\cdot10^{-2}$		$1.26\cdot10^{-4}$	$1.45\cdot10^{-4}$	$1.24\cdot10^{-2}$		
705	$1.52\cdot10^{-2}$		$1.28\cdot10^{-3}$	$1.18\cdot10^{-3}$	$2.84\cdot10^{-2}$	$3.89\cdot10^{-5}$	$3.99\cdot10^{-5}$
762	$3.08\cdot10^{-2}$	$1.58\cdot10^{-2}$	$1.36\cdot10^{-2}$	$6.65\cdot10^{-3}$	$6.10\cdot10^{-2}$	$1.67\cdot10^{-4}$	$2.19\cdot10^{-4}$
808	$1.55\cdot10^{-2}$	$5.65\cdot10^{-2}$	$4.68\cdot10^{-2}$	$1.75\cdot10^{-2}$	$7.61\cdot10^{-2}$	$3.04\cdot10^{-4}$	$4.51\cdot10^{-4}$
855	$1.13\cdot10^{-2}$	$8.89\cdot10^{-2}$	$2.86\cdot10^{-2}$	$2.39\cdot10^{-2}$	$9.29\cdot10^{-2}$	$1.40\cdot10^{-4}$	$2.93\cdot10^{-4}$
897	$3.28\cdot10^{-3}$	$1.40\cdot10^{-1}$	$2.64\cdot10^{-2}$	$2.48\cdot10^{-2}$	$1.80\cdot10^{-1}$	$3.34\cdot10^{-4}$	$2.10\cdot10^{-3}$
935	$5.65\cdot10^{-4}$	$1.79\cdot10^{-1}$	$1.24\cdot10^{-2}$	$1.25\cdot10^{-2}$	$9.90\cdot10^{-2}$	$2.54\cdot10^{-4}$	$2.39\cdot10^{-3}$
986	$4.79\cdot10^{-3}$	$1.69\cdot10^{-1}$	$8.93\cdot10^{-3}$	$7.03\cdot10^{-3}$	$7.77\cdot10^{-2}$	$3.44\cdot10^{-4}$	$4.02\cdot10^{-3}$
1039	$1.44\cdot10^{-3}$	$9.80\cdot10^{-2}$	$5.89\cdot10^{-3}$	$4.50\cdot10^{-3}$	$6.30\cdot10^{-2}$	$3.92\cdot10^{-4}$	$3.82\cdot10^{-3}$
1077	$4.09\cdot10^{-3}$	$7.08\cdot10^{-2}$	$3.46\cdot10^{-3}$	$4.13\cdot10^{-3}$	$7.51\cdot10^{-2}$	$4.09\cdot10^{-4}$	$2.34\cdot10^{-3}$
1133	$2.97\cdot10^{-3}$	$5.70\cdot10^{-2}$	$1.55\cdot10^{-3}$	$3.94\cdot10^{-3}$	$6.40\cdot10^{-2}$	$4.66\cdot10^{-4}$	$1.78\cdot10^{-3}$
1173	$6.76\cdot10^{-4}$	$2.89\cdot10^{-2}$	$4.84\cdot10^{-4}$	$3.37\cdot10^{-3}$	$4.55\cdot10^{-2}$	$3.14\cdot10-4$	$9.43\cdot10^{-4}$
1223	$8.30\cdot10^{-4}$	$2.00\cdot10^{-2}$	$1.36\cdot10^{-4}$	$3.55\cdot10^{-3}$	$4.62\cdot10^{-2}$	$1.91\cdot10^{-4}$	$4.05\cdot10^{-4}$
1253		$1.70\cdot10^{-2}$	$5.11\cdot10^{-5}$	$5.02\cdot10^{-3}$	$7.95\cdot10^{-2}$	$1.57\cdot10^{-4}$	$2.24\cdot10^{-4}$
1290		$1.03\cdot10^{-2}$	$3.25\cdot10^{-5}$	$3.00\cdot10^{-3}$	$7.12\cdot10^{-4}$	$7.70\cdot10^{-5}$	$8.23\cdot10^{-5}$
Total	$1.75\cdot10^{-1}$	$9.51\cdot10^{-1}$	$1.50\cdot10^{-1}$	$1.22\cdot10^{-1}$	$2.47\cdot10^{-2}$	$3.59\cdot10^{-3}$	$1.91\cdot10^{-2}$

Pyrolysis Temperature (K)	Molar yields (mmol)						
	C_3H_6	C_3H_8	C_4H_8	C_4H_{10}	C_6H_6	C_7H_8	C_8H_{10}
320							
364							
415							
463							
511							
556							
610							
654							
705	$9.65\cdot10^{-6}$	$3.73\cdot10^{-6}$			$3.15\cdot10^{-5}$	$7.96\cdot10^{-5}$	$1.42\cdot10^{-5}$
762	$4.33\cdot10^{-5}$	$1.90\cdot10^{-5}$			$5.83\cdot10^{-4}$	$1.05\cdot10^{-3}$	$4.78\cdot10^{-4}$
808	$4.16\cdot10^{-5}$	$2.17\cdot10^{-5}$			$1.05\cdot10^{-3}$	$1.70\cdot10^{-3}$	$4.36\cdot10^{-4}$
855	$1.62\cdot10^{-5}$	$2.12\cdot10^{-5}$		$5.54\cdot10^{-6}$	$3.46\cdot10^{-4}$	$7.47\cdot10^{-5}$	$1.52\cdot10^{-5}$
897	$2.09\cdot10^{-4}$	$6.42\cdot10^{-4}$	$2.85\cdot10^{-5}$	$9.72\cdot10^{-5}$	$7.61\cdot10^{-5}$	$2.86\cdot10^{-5}$	
935	$2.96\cdot10^{-4}$	$1.05\cdot10^{-3}$	$5.62\cdot10^{-5}$	$2.02\cdot10^{-4}$	$7.78\cdot10^{-5}$	$2.10\cdot10^{-5}$	
986	$2.68\cdot10^{-4}$	$1.09\cdot10^{-3}$	$6.34\cdot10^{-5}$	$2.12\cdot10^{-4}$	$3.14\cdot10^{-5}$	$7.73\cdot10^{-6}$	
1039	$4.27\cdot10^{-4}$	$1.22\cdot10^{-3}$	$6.62\cdot10^{-5}$	$2.21\cdot10^{-4}$	$2.67\cdot10^{-5}$	$7.31\cdot10^{-6}$	
1077	$4.31\cdot10^{-4}$	$1.15\cdot10^{-3}$	$7.76\cdot10^{-5}$	$1.85\cdot10^{-4}$	$7.79\cdot10^{-5}$	$2.25\cdot10^{-5}$	
1133	$3.19\cdot10^{-4}$	$8.52\cdot10^{-4}$	$6.39\cdot10^{-5}$	$1.16\cdot10^{-4}$	$4.06\cdot10^{-5}$	$1.01\cdot10^{-5}$	
1173	$2.06\cdot10^{-4}$	$3.60\cdot10^{-4}$	$3.64\cdot10^{-5}$	$5.91\cdot10^{-5}$	$4.44\cdot10^{-5}$	$1.10\cdot10^{-5}$	
1223	$1.30\cdot10^{-4}$	$1.68\cdot10^{-4}$	$2.56\cdot10^{-5}$	$3.09\cdot10^{-5}$	$3.36\cdot10^{-5}$	$5.36\cdot10^{-6}$	
1253	$1.39\cdot10^{-4}$	$1.09\cdot10^{-4}$	$1.92\cdot10^{-5}$	$2.60\cdot10^{-5}$	$9.40\cdot10^{-6}$	$7.16\cdot10^{-6}$	
1290	$8.84\cdot10^{-5}$	$5.84\cdot10^{-5}$	$1.47\cdot10^{-5}$	$1.49\cdot10^{-5}$	$3.56\cdot10^{-6}$	$4.73\cdot10^{-6}$	
Total	$2.62\cdot10^{-3}$	$6.76\cdot10^{-3}$	$4.52\cdot10^{-4}$	$1.17\cdot10^{-3}$	$2.43\cdot10^{-3}$	$3.02\cdot10^{-3}$	$9.43\cdot10^{-4}$

Pyrolysis temperature (K)	Molar yields (mmol)			
	C_6H_6O	C_7H_8O	$C_8H_{10}O$	$C_9H_{12}O$
320				
364				
415	$9.25\cdot10^{-5}$			
463	$1.98\cdot10^{-4}$			
511	$4.93\cdot10^{-5}$			
556	$9.52\cdot10^{-5}$	$2.52\cdot10^{-5}$		
610	$2.18\cdot10^{-3}$	$9.56\cdot10^{-4}$	$1.31\cdot10^{-4}$	
654	$3.48\cdot10^{-3}$	$2.95\cdot10^{-3}$	$7.25\cdot10^{-4}$	$2.51\cdot10^{-5}$
705	$5.78\cdot10^{-3}$	$6.72\cdot10^{-3}$	$2.05\cdot10^{-3}$	$8.98\cdot10^{-5}$
762	$8.64\cdot10^{-3}$	$9.08\cdot10^{-3}$	$2.38\cdot10^{-3}$	$9.13\cdot10^{-5}$
808	$3.28\cdot10^{-3}$	$2.24\cdot10^{-3}$	$3.66\cdot10^{-4}$	$7.71\cdot10^{-6}$
855	$1.39\cdot10^{-4}$	$6.73\cdot10^{-5}$		
897	$4.84\cdot10^{-5}$	$6.99\cdot10^{-6}$		
935	$1.45\cdot10^{-5}$			
986	$2.84\cdot10^{-6}$			
1039				
1077				
1133				
1173				
1223				
1253				
1290				
Total	$2.40\cdot10^{-2}$	$2.21\cdot10^{-2}$	$5.66\cdot10^{-3}$	$2.14\cdot10^{-4}$

Table 2
Mass yields of pyrolysis products versus pyrolysis temperature.

Pyrolysis temperature (K)	Mass yields (mg)						
	H_2O	H_2	CH_4	CO	CO_2	C_2H_4	C_2H_6
320	$2.57\cdot10^{-1}$				$8.63\cdot10^{-3}$		
364	$1.74\cdot10^{-1}$				$2.83\cdot10^{-3}$		
415	$1.02\cdot10^{-1}$				$8.27\cdot10^{-3}$		
463	$6.92\cdot10^{-2}$		$2.62\cdot10^{-4}$	$8.86\cdot10^{-4}$	$7.45\cdot10^{-3}$		
511	$1.18\cdot10^{-1}$		$2.48\cdot10^{-4}$	$4.74\cdot10^{-3}$	$3.77\cdot10^{-3}$		
556	$8.99\cdot10^{-2}$		$4.10\cdot10^{-4}$	$4.12\cdot10^{-3}$	$7.63\cdot10^{-3}$		
610	$1.74\cdot10^{-1}$		$1.15\cdot10^{-3}$	$2.58\cdot10^{-3}$	$1.67\cdot10^{-2}$		
654	$5.24\cdot10^{-1}$		$2.03\cdot10^{-3}$	$4.07\cdot10^{-3}$	$1.24\cdot10^{-2}$		
705	$2.74\cdot10^{-1}$		$2.05\cdot10^{-2}$	$3.30\cdot10^{-2}$	$2.84\cdot10^{-2}$	$1.09\cdot10^{-3}$	$1.20\cdot10^{-3}$
762	$5.55\cdot10^{-1}$	$3.18\cdot10^{-2}$	$2.18\cdot10^{-1}$	$1.86\cdot10^{-1}$	$6.10\cdot10^{-2}$	$4.68\cdot10^{-3}$	$6.59\cdot10^{-3}$
808	$2.78\cdot10^{-1}$	$1.14\cdot10^{-1}$	$7.51\cdot10^{-1}$	$4.90\cdot10^{-1}$	$7.61\cdot10^{-2}$	$8.53\cdot10^{-3}$	$1.36\cdot10^{-2}$
855	$2.04\cdot10^{-1}$	$1.79\cdot10^{-1}$	$4.58\cdot10^{-1}$	$6.70\cdot10^{-1}$	$9.29\cdot10^{-2}$	$3.93\cdot10^{-3}$	$8.81\cdot10^{-3}$
897	$5.91\cdot10^{-2}$	$2.82\cdot10^{-1}$	$4.24\cdot10^{-1}$	$6.94\cdot10^{-1}$	$1.80\cdot10^{-1}$	$9.37\cdot10^{-3}$	$6.32\cdot10^{-2}$
935	$1.02\cdot10^{-2}$	$3.60\cdot10^{-1}$	$2.00\cdot10^{-1}$	$3.50\cdot10^{-1}$	$9.90\cdot10^{-2}$	$7.12\cdot10^{-3}$	$7.17\cdot10^{-2}$
986	$8.63\cdot10^{-2}$	$3.41\cdot10^{-1}$	$1.43\cdot10^{-1}$	$1.97\cdot10^{-1}$	$7.77\cdot10^{-2}$	$9.64\cdot10^{-3}$	$1.21\cdot10^{-1}$
1039	$2.60\cdot10^{-2}$	$1.98\cdot10^{-1}$	$9.45\cdot10^{-2}$	$1.26\cdot10^{-1}$	$6.30\cdot10^{-2}$	$1.10\cdot10^{-2}$	$1.15\cdot10^{-1}$
1077	$7.36\cdot10^{-2}$	$1.43\cdot10^{-1}$	$5.54\cdot10^{-2}$	$1.16\cdot10^{-1}$	$7.51\cdot10^{-2}$	$1.15\cdot10^{-2}$	$7.04\cdot10^{-2}$
1133	$5.35\cdot10^{-2}$	$1.15\cdot10^{-1}$	$2.48\cdot10^{-2}$	$1.10\cdot10^{-1}$	$6.41\cdot10^{-2}$	$1.31\cdot10^{-2}$	$5.34\cdot10^{-2}$
1173	$1.22\cdot10^{-2}$	$5.84\cdot10^{-2}$	$7.77\cdot10^{-3}$	$9.43\cdot10^{-2}$	$4.55\cdot10^{-2}$	$8.81\cdot10^{-3}$	$2.84\cdot10^{-2}$
1223	$1.50\cdot10^{-2}$	$4.02\cdot10^{-2}$	$2.18\cdot10^{-3}$	$9.95\cdot10^{-2}$	$4.62\cdot10^{-2}$	$5.37\cdot10^{-3}$	$1.22\cdot10^{-2}$
1253		$3.43\cdot10^{-2}$	$8.21\cdot10^{-4}$	$1.41\cdot10^{-1}$	$7.95\cdot10^{-2}$	$4.41\cdot10^{-3}$	$6.74\cdot10^{-3}$
1290		$2.07\cdot10^{-2}$	$5.21\cdot10^{-4}$	$8.41\cdot10^{-2}$	$3.14\cdot10^{-2}$	$2.16\cdot10^{-3}$	$2.47\cdot10^{-3}$
Total	3.153	1.917	2.404	3.408	1.087	0.101	0.574

Pyrolysis Temperature (K)	Mass yields (mg)						
	C_3H_6	C_3H_8	C_4H_8	C_4H_{10}	C_6H_6	C_7H_8	C_8H_{10}
320							
364							
415							
463							
511							
556							
610							
654							
705	$4.06\cdot10^{-4}$	$1.65\cdot10^{-4}$			$2.46\cdot10^{-3}$	$7.33\cdot10^{-3}$	$1.51\cdot10^{-3}$
762	$1.82\cdot10^{-3}$	$8.37\cdot10^{-4}$			$4.56\cdot10^{-2}$	$9.63\cdot10^{-2}$	$5.07\cdot10^{-2}$
808	$1.75\cdot10^{-3}$	$9.58\cdot10^{-4}$			$8.21\cdot10^{-2}$	$1.56\cdot10^{-1}$	$4.63\cdot10^{-2}$
855	$6.83\cdot10^{-4}$	$9.34\cdot10^{-4}$		$3.22\cdot10^{-4}$	$2.70\cdot10^{-2}$	$6.88\cdot10^{-3}$	$1.61\cdot10^{-3}$
897	$8.80\cdot10^{-3}$	$2.83\cdot10^{-2}$	$1.60\cdot10^{-3}$	$5.65\cdot10^{-3}$	$5.94\cdot10^{-3}$	$2.63\cdot10^{-3}$	
935	$1.25\cdot10^{-2}$	$4.63\cdot10^{-2}$	$3.15\cdot10^{-3}$	$1.17\cdot10^{-2}$	$6.08\cdot10^{-3}$	$1.94\cdot10^{-3}$	
986	$1.13\cdot10^{-2}$	$4.79\cdot10^{-2}$	$3.56\cdot10^{-3}$	$1.23\cdot10^{-2}$	$2.45\cdot10^{-3}$	$7.12\cdot10^{-4}$	
1039	$1.80\cdot10^{-2}$	$5.37\cdot10^{-2}$	$3.71\cdot10^{-3}$	$1.29\cdot10^{-2}$	$2.09\cdot10^{-3}$	$6.73\cdot10^{-4}$	
1077	$1.82\cdot10^{-2}$	$5.08\cdot10^{-2}$	$4.36\cdot10^{-3}$	$1.08\cdot10^{-2}$	$6.08\cdot10^{-3}$	$2.08\cdot10^{-3}$	
1133	$1.34\cdot10^{-2}$	$3.76\cdot10^{-2}$	$3.59\cdot10^{-3}$	$6.73\cdot10^{-3}$	$3.17\cdot10^{-3}$	$9.34\cdot10^{-4}$	
1173	$8.65\cdot10^{-2}$	$1.59\cdot10^{-2}$	$2.04\cdot10^{-3}$	$3.44\cdot10^{-3}$	$3.47\cdot10^{-3}$	$1.01\cdot10^{-3}$	
1223	$5.49\cdot10^{-3}$	$7.40\cdot10^{-3}$	$1.44\cdot10^{-3}$	$1.79\cdot10^{-3}$	$2.62\cdot10^{-3}$	$4.97\cdot10^{-4}$	
1253	$5.85\cdot10^{-3}$	$4.81\cdot10^{-3}$	$1.08\cdot10^{-3}$	$1.51\cdot10^{-3}$	$7.34\cdot10^{-4}$	$6.60\cdot\cdot10^{-4}$	
1290	$3.72\cdot10^{-3}$	$2.58\cdot10^{-3}$	$8.26\cdot10^{-4}$	$8.64\cdot10^{-4}$	2.7810^{-4}	$4.36\cdot10^{-4}$	
Total	0.110	0.298	0.025	0.068	0.190	0.279	0.100

Pyrolysis Temperature (K)	Mass yields (mg)			
	C_6H_6O	C_7H_8O	$C_8H_{10}O$	$C_9H_{12}O$
320				
364				
415	$8.70\cdot10^{-3}$			
463	$1.86\cdot10^{-2}$			
511	$4.64\cdot10^{-3}$			
556	$8.96\cdot10^{-3}$	$2.73\cdot10^{-3}$		
610	$2.05\cdot10^{-1}$	$1.03\cdot10^{-1}$	$1.60\cdot10^{-2}$	
654	$3.27\cdot10^{-1}$	$3.19\cdot10^{-1}$	$8.85\cdot10^{-2}$	$3.41\cdot10^{-3}$
705	$5.44\cdot10^{-1}$	$7.27\cdot10^{-1}$	$2.51\cdot10^{-1}$	$1.22\cdot10^{-2}$
762	$8.13\cdot10^{-1}$	$9.82\cdot10^{-1}$	$2.91\cdot10^{-1}$	$1.24\cdot10^{-2}$
808	$3.09\cdot10^{-1}$	$2.42\cdot10^{-1}$	$4.47\cdot10^{-2}$	$1.05\cdot10^{-3}$
855	$1.31\cdot10^{-2}$	$7.28\cdot10^{-3}$		
897	$4.55\cdot10^{-3}$	$7.56\cdot10^{-4}$		
935	$1.36\cdot10^{-3}$			
986	$2.67\cdot10^{-4}$			
1039				
1077				
1133				
1173				
1223				
1253				
1290				
Total	2.258	2.384	0.691	0.029

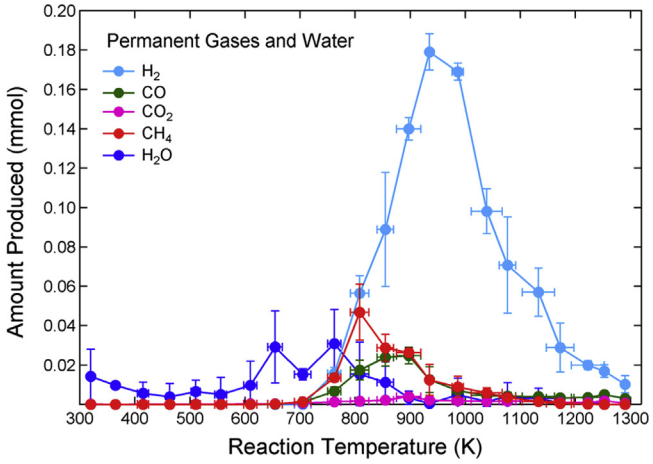

Fig. 11. The amount of permanent gases produced from phenol-formaldehyde resin pyrolysis as a function of reaction (sample) temperature.

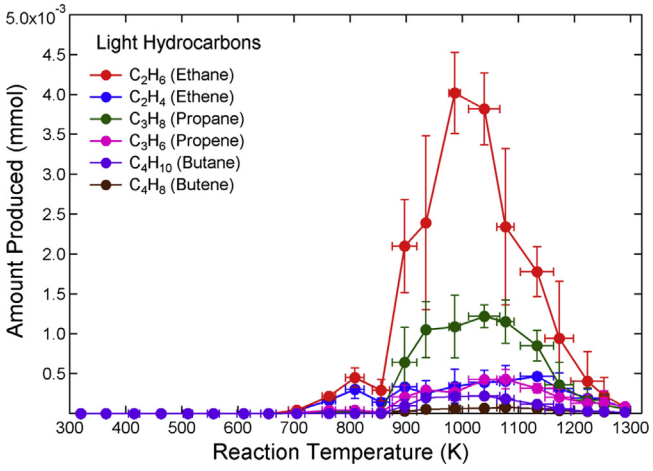

Fig. 12. The amount of light hydrocarbons produced from phenol-formaldehyde resin pyrolysis as a function of reaction (sample) temperature.

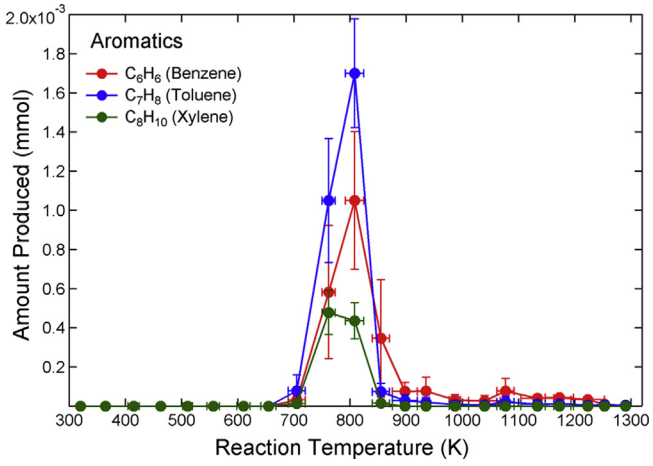

Fig. 13. The amount of aromatic compounds produced from phenol-formaldehyde resin pyrolysis as a function of reaction (sample) temperature.

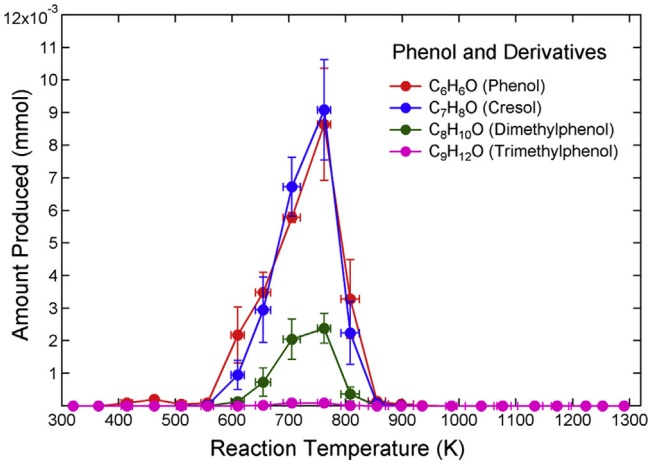

Fig. 14. The amount of aromatic alcohols produced from phenol-formaldehyde resin pyrolysis as a function of reaction (sample) temperature.

- Yields of aromatic products, including benzene, toluene, and xylene, are only significant between 700 and 850 K;
- Permanent gases such as hydrogen, methane, carbon monoxide, and carbon dioxide are mostly produced between 800 K and 1200 K;
- The yields of light hydrocarbons peak at 1000 K, although their yields are very minor compared to permanent gases.

Our results are consistent with available experimental findings and the widely accepted three stage pyrolysis mechanism. However, our work provides more quantitative details than previous experiments, which can be further used to develop a more comprehensive chemical kinetic model deducing detailed reaction pathways of phenol-formaldehyde resin pyrolysis.

Acknowledgments

This research was originally funded by NASA's Fundamental Aeronautic Program Hypersonics NRA grant NNX12AG47A. It is currently supported by the Space Technology Research Grants Program under the same grant number. The authors would like to thank B. Helber, G. Glabeke, T. Magin, J.-B. Gouriet and O. Chazot at the von Karman Institute (VKI) for Fluid Dynamics for their support and collaboration with the TGA measurements.

Appendix A. Supplementary data

Supplementary data related to this article can be found at http://dx.doi.org/10.1016/j.polymdegradstab.2014.12.020.

References

[1] Trick KA, Saliba TE. Mechanisms of the pyrolysis of phenolic resin in a carbon/phenolic composite. Carbon 1995;33(11):1509–15.
[2] Trick KA, Saliba TE, Sandhu SS. A kinetic model of the pyrolysis of phenolic resin in a carbon/phenolic composite. Carbon 1997;35(3):393–401.
[3] Jiang H, Wang J, Wu S, Wang B, Wang Z. Pyrolysis kinetics of phenol-formaldehyde resin by non-isothermal thermogravimetry. Carbon 2010;48:1527–33.
[4] Jiang H, Wang J, Wu S, Yuan Z, Hu Z, Wu R, et al. The pyrolysis mechanism of phenol formaldehyde resin. Polym Degrad Stab 2012;97:1527–33.
[5] B. S. Venkatachari, G. C. Cheng, R. P. Koomullil, A. Ayasoufi. Computational tools for re-entry aerothermodynamics: Part II. Surf ablation. AIAA paper 2008–1218.
[6] N. N. Mansour, J. Lachaud, T. E. Magin, J. de Muelenaere, Y.-K. Chen. High-fidelity charring ablator thermal response model. AIAA Pap 2011–3124.
[7] Y.-K. Chen, F. Milos. Effects of non-equilibrium chemistry and darcy-forchheimer flow of pyrolysis gas for a charring ablator. AIAA Pap 2011–3122.

[8] A. Bennett, D. R. Payne, R. W. Court. Quantitative pyrolytic and elemental analysis of a phenolic resin. AIAA Pap 2013–0183.
[9] H.-W. Wong, J. Peck, R. A. Edwards, G. Reinisch, J. Lachaud, N. N. Mansour. Measurement of pyrolysis products from phenolic polymer thermal decomposition. AIAA Pap 2014-1388.
[10] Suuberg EM, Wojtowicz M, Calo JM. Some aspects of the thermal annealing process in a phenol-formaldehyde resin char. Carbon 1989;27(3):430–41.
[11] Chetan MS, Ghadage RS, Rajan CR, Gunjikar VG. Thermolysis of orthonovolacs. part 1. phenol-formaldehyde and m-cresol formaldehyde resins. Thermochim Acta 1993;228:261–70.
[12] Costa L, de Montelera LR, Camino G, Weil ED, Pearce EM. Structure-charring relationship in phenol-formaldehyde type resins. Polym Degrad Stab 1997;56:23–35.
[13] Lytle CA, Bertsch W, McKinley M. Determination of novolac resin thermal decomposition products by pyrolysis-gas chromatography. J Anal Appl Pyrolysis 1998;45:121–31.
[14] Rao MPR, Rao BSM, Rajan CR, Ghadage RS. Thermal degradation kinetics of phenol-formaldehyde resins. Polym Degrad Stab 1998;61:283–8.
[15] Lin J-M, Ma C-CM. Thermal degradation of phenolic resin/silica hybrid beramers. Polym Degrad Stab 2000;69:229–35.
[16] Ouchi K. Infra-red study of structural changes during the pyrolysis of a phenol-formaldehyde resin. Carbon 1966;4:59–66.
[17] Yamashita Y, Ouchi K. A study on carbonization of phenol-formaldehyde resin labelled with deuterium and c13. Carbon 1981;19:89–94.
[18] Morterra C, Low MJD. Ir studies of carbons – vii. the pyrolysis of a phenol-formaldehyde resin. Carbon 1985;23(5):525–30.
[19] Lausevic Z, Marinkovic S. Mechanical properties and chemistry of carbonization of phenol formaldehyde resin. Carbon 1986;24(5):575–80.
[20] Alonso MV, Oliet M, Dominguez JC, Rojo E, Rodriguez F. Thermal degradation of lignin-phenol-formaldehyde and phenol-formaldehyde resol resins. J Therm Analysis Calorim 2011;105:349–56.
[21] Sykes GF. Decomposition characteristics of a char-forming phenolic polymer used for ablative composites. Technical report. NASA; 1967.
[22] Sykes GF. Thermal cracking of phenolic-nylon pyrolysis products on passing through a heated char. Technical report. NASA; 1970.
[23] Lum R, Wilkins W, Robbins M, Lyons AM, Jones RP. Thermal analysis of graphite and carbon-phenolic composites by pyrolysis-mass spectrometry. Carbon 1983;21(2):111–6.
[24] Hetper J, Sobera M. Thermal degradation of novolac resins by pyrolysis-gas chromatography with a movable reaction zone. J Chromatogr A 1999;833:277–81.
[25] Grenier-Loustalot M-F, Raffin G, Salino B, Paisse O. Phenolic resins part 6. identifications of volatile organic molecules during thermal treatment of neat resols and resol filled with glass fibers. Polymer 2000;41:7123–32.
[26] Sobera M, Hetper J. Pyrolysis-gas chromatography-mass spectrometry of cured phenolic resins. J Chromatogr A 2003;993:131–5.